# Arbitrary Wireless Energy Distribution within an Epsilon Near-zero Environment

Yang, Qingdong; Wang, Yi; Shi, Jinhui; Liu, Changxu; Zhang, Shuang

*DOI:*
10.1002/lpor.202300631
10.1002/lpor.v18.2

# Arbitrary Wireless Energy Distribution within an Epsilon Near-zero Environment

*Qingdong Yang, Yi Wang, Jinhui Shi, Changxu Liu,* and Shuang Zhang**

**Efficient power distribution to multiple receivers with controlled amounts is critical for wireless communication and sensing systems. Previous efforts have attempted to improve power transfer efficiency through strong coupling and parity-time (PT) symmetry, providing attractive opportunities for flexible energy flow control. In this study, a novel method for achieving arbitrary power distribution is proposed and numerically demonstrated by leveraging the unique properties inside an epsilon near-zero (ENZ) environment. Specifically, it shows that the power from a single source can be transferred to multiple receivers inside an ENZ medium with negligible loss by modifying optical properties of receivers rather than introducing sophisticated active control modules. Importantly, full power transfer is independent of the size and shape of the ENZ medium, as well as the positions of the receivers and source. A realizable system is further designed with effective zero index at microwave frequencies to confirm the high efficiency of energy transfer. The innovative approach, employing photonic doping for advanced and efficient wireless power transfer, may shed light on the new generation of energy efficient communication/sensing systems with versatile control functionalities.**

## 1. Introduction

Since Nikola Tesla first proposed the idea of wireless power transfer (WPT),[1] it has been playing a central role in both practical applications and fundamental research, especially in radiofrequency-related fields such as consumer electronics, medical devices and automotive applications.[2–5] As the demand for better efficiency and controllability increases, traditional WPT methods face compromises between efficiency, stability, and cost,[6,7] limiting their widespread adoption. Several solutions have been proposed to partially solve the aforementioned problem in recent years. Resonance based WPT is proposed to increase the coupling efficiency at mid-range distance between strongly coupled resonators.[8] PT-symmetric configurations provide robust to variations in coupling when distance is changed.[9–12] Self-oscillating WPT is beneficial for no additional tuning circuitry to realize robust operation.[13,14] Moreover, adding metamaterials of negative permeability in a WPT system is another way to improve energy transfer efficiency which is more compatible and miniaturized.[15–17] Some metamaterials techniques are more precious to control the transmission directions.[18,19] Epsilon near-zero index (ENZ) materials have gained enormous momentum for decades, fertilizing many disciplines in photonics.[20–27] Among the intriguing phenomena associated with ENZ materials, supercoupling[28–30] stands out, enabling robust energy tunneling of electromagnetic waves against deformations of waveguides. Consequently, supercoupling has been proposed for various applications, such as waveguide interconnects,[31] cloaking,[32] nonlinear effect,[33] and quantum emission.[34] Besides, ENZ metamaterials have been reported

Q. Yang, S. Zhang
Department of Physics
The University of Hong Kong
Hong Kong 999077, China
E-mail: shuzhang@hku.hk

Y. Wang
Department of Electronic, Electrical and Systems Engineering
University of Birmingham
Birmingham B15 2TT, UK

J. Shi
College of Physics and Optoelectronic Engineering
Harbin Engineering University
Harbin 130407, China

C. Liu
Centre for Metamaterial Research & Innovation, Department of Engineering
University of Exeter
Exeter EX4 4QF, UK
E-mail: c.c.liu@exeter.ac.uk

S. Zhang
Department of Electronic, Electrical Engineering
The University of Hong Kong
Hong Kong 999077, China

S. Zhang
New Cornerstone Science Laboratory, Department of Physics
The University of Hong Kong
Hong Kong 999077, China

The ORCID identification number(s) for the author(s) of this article can be found under https://doi.org/10.1002/lpor.202300631



**DOI: 10.1002/lpor.202300631**

to provide a limited efficiency improvement by amplification of near-field.[35–37] However, the investigation of WPT inside ENZ materials remains elusive, leaving an open question regarding how the potential of ENZ can be fully explored for WPT.

Here, we propose a novel implementation of wireless power transfer with negligible loss inside ENZ environment, allowing for arbitrary power distribution. We reveal that the efficiency of power transfer remains near 100% for any arbitrary shape of an ENZ material, with minimal power leakage into open space, regardless of the distance between the emitter and the receiver. Notably, we unveil that the transfer efficiency at the receiver is determined by its own properties and is independent of the resonance of the emitter. We verify the above transmission properties through both an analytical model and full-wave simulations within an ideal ENZ material. The transmission properties are protected by the ENZ condition, independent of specific geometric parameters and immune to perturbations and inter-couplings that preserve the required ENZ condition. We further show that it is possible to distribute power among multiple receivers flexibly, using a passive approach that significantly reduces the complexity of the system. Our explorations may extend applications in the rapidly growing fields of WPT, opening up new opportunities for a wide range of electromagnetic systems that require robust and efficient functionalities.

## 2. Theory of Full Energy Transfer in the ENZ Limt

To describe how ENZ materials can lead to a robust and highly efficient transfer scheme, we consider a general scenario, which is schematically depicted in **Figure 1**a, in which a source resonator and a receiver resonator are immersed in a 2D ENZ body of an arbitrary shape, identified as S-rod and R-rod, respectively. To simplify the analysis, we model the source as a magnetic dipole along the z direction in a dielectric medium, and use a lossy medium to simulate the receiver. We solve the problem by using the doping theory,[38] which is originally developed for adjusting the permeability of materials with near zero permittivity. We find that one of the unique features of ENZ medium - the uniform distribution of magnetic field, persists when the source and receiver are immersed in the ENZ material (see details in Supporting Information). Interestingly, the magnetic field is solely determined by the shape and dielectric parameter of the medium, and is independent of positions of S-rod and R-rod. This position-independence indicates that the coupling strength between rods is invariant at difference distances, and it leads to invariant power transfer even when the distance between them changes inside the ENZ medium. This property provides a platform to achieve highly efficient wireless energy transfer.

Now, we will demonstrate how to obtain distance-independent transfer of energy between the source and receiver. We begin with the calculation of the power that is leaked into air and the power that is transferred to the R-rod by using the Poynting theorem $P = \oint_{\partial A} \frac{1}{2}\,\mathrm{Re}(E \times H^{*})dl$, where the integration is performed over the boundaries of ENZ materials and R-rod, respectively. Considering the uniform magnetic field inside the ENZ ($H_z$) and the field on the boundary of S-rod $H_z\psi_{R\text{-}rod}$, where $\psi_{R\text{-}rod}$ is the solution to scalar Helmholtz equation at the boundary of R-rod (detailed form in Supporting Information), the energy transfer in the rod can be calculated using the formula $P_{\text{transfer}} = |H_Z|^2 \oint_{\partial A} \frac{1}{2}\,\mathrm{Re}(\frac{1}{i\omega\epsilon_2}\psi^{*}_{\text{R-rod}} \nabla \times \psi_{\text{R-rod}}\vec{e_z})dl$.

Similarly, we can express the energy loss as $P_{\text{loss}} = |H_Z|^2 \oint_{\partial A} \frac{1}{2}\,\mathrm{Re}(\frac{1}{i\omega\epsilon_0}\psi^{*}_{\text{air}} \nabla \times \psi_{\text{air}}\vec{e_z})$ where $\psi_{air}$ is the solution to scalar Helmholtz equation on the boundary of ENZ material. Due to the uniform distribution of the magnetic field in ENZ region, both the power received by the R-rod and the power leakage into air is proportional to $|H_z|^2$. This means that for a given shape of ENZ medium ($\psi_{air}$ is invariant), the field on the boundary of R-rod ($\psi_{R\text{-}rod}$ ) determines the ratio of energy transfer. Thus, the theoretical analysis outlined above indicates that to achieve complete energy transfer, we need to maximize the field inside R-rod to minimize the dissemination of the power in air. Hence, inducing a strong field enhancement inside the R-rod through resonance effect appears to be a viable solution for achieving complete energy transfer, considering the efficiency $\eta = \frac{P_{\text{transfer}}}{P_{\text{transfer}} + P_{\text{loss}}}$.

As a case study, we consider the configuration in Figure 1a, in which the radius of S-rod ($r_1$) and R-rod ($r_2$) are both $0.122\lambda$, and the ENZ region has the shape of a circle with a radius of $13r_1$ ($R_{enz}$) and a relative permittivity of 0.0001 ($\epsilon_{enz}$), where $\lambda$ is

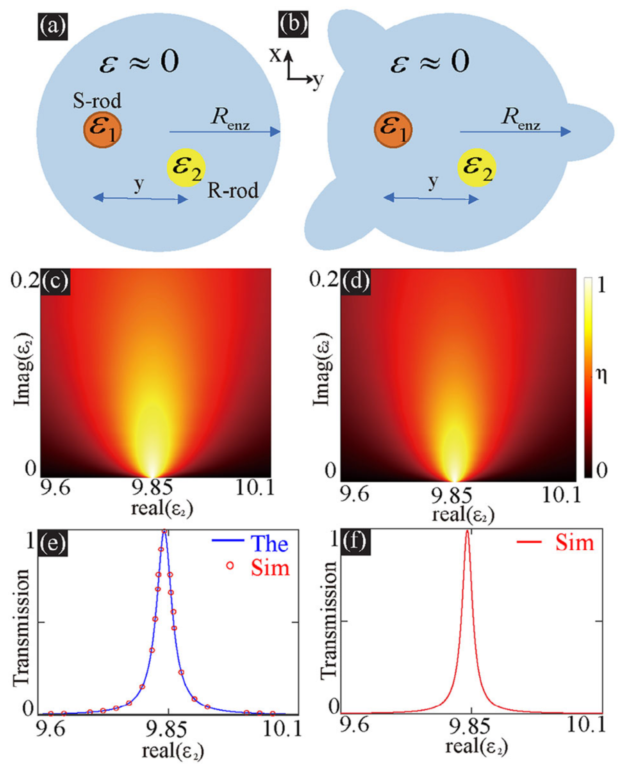


**Figure 1.** Illustration of the robust and highly efficient transfer inside ENZ materials. a,b) Sketch of the geometry configuration: a 2D arbitrary shape of ENZ material. Inside the ENZ, the ideal source and receiver are presented by two circles with different permittivity $\epsilon_1$ and $\epsilon_2$ respectively (radius r). The magnetic dipole along z-axis is placed at the center of S-rod to excited the wave. c,d) Dependence of transmission on the permittivity of R-rod for the different shape of ENZ in (a,b), respectively. The x and y axis represent the real and image part of the permittivity, respectively. e,f) Transmission spectrum for $\mathbf{Im}(\epsilon_2) = 0.0016$ for the configuration in (a,b). 'The' represents theory and 'Sim' represents simulation.

the working wavelength in free space. With this configuration the field can be solved analytically based on the Helmholtz equation. Direct calculation of the magnetic field inside the R-rod yields $\psi_{\text{loss}}(\mathbf{r}) = J_0(k_2\mathbf{r})/J_0(k_2r_2)$, where $J_n$ and $k_2$ represent the cylindrical Bessel function of order n and the wave number in $\epsilon_2$, respectively. The power transfer into the R-rod is given as

$$P_{\text{transfer}} = \text{Re}\left[\frac{\pi r_2}{i\omega\epsilon_2}\frac{k_2 J_1(k_2r_2)}{J_0(k_2r_2)}|Hz|^2\right] \quad (1)$$

Similarly, outside the ENZ region, the distribution of field is given by $\psi_{\text{air}}(\mathbf{r}) = H_0(k_0\mathbf{r})/H_0(k_0R_{\text{enz}})$, where $H_n$ represents the cylindrical Hankel function of order n. The energy loss in the air is thus expressed as

$$P_{\text{loss}} = \text{Re}\left[\frac{\pi R_{enz}}{iw\epsilon_0}\frac{k_0 H_1(k_0R_{enz})}{H_0(k_0R_{enz})}|Hz|^2\right] \quad (2)$$

From Equation (1), resonant behavior occurs at $J_0(k_2r_2) = 0$ when $k_2$ is real, corresponding to a lossless dielectric rod. However, when the dielectric rod becomes lossy, $J_0(k_2r_2)$ would have no zeros. Nonetheless, the resonance still occurs at the original lossless dielectric parameter. Under the condition of resonance, the field inside R-rod is much stronger than at other locations, indicating that $P_{\text{loss}}$ is much smaller than $P_{\text{transfer}}$, allowing for near unity energy transfer.

For the given geometric parameters shown in Figure 1a, the influence of complex permittivity of R-rod on the energy transmission is illustrated by Figure 1c, which shows the transmission plotted against the real (x-axis) and imaginary (y-axis) parts of $\epsilon_2$, respectively. As we predicted, nearly complete transmission occurs at resonance ($\epsilon_2$=9.843+0.0016i). It is important to note that the resonance persists within a narrow range around the designed parameters. As a result, the efficiency of energy transfer is more than 80% in the relatively large range for the real part of the permittivity. However, far from the resonance condition, the efficiency drops significantly. We validate our results via numerical simulations based on Comsol Multiphysics with a fixed imaginary part of permittivity (**Im**$\epsilon_2$=0.0016). The numerical results, as shown in Figure 1c, agree well with the analytical studies. Because the ratio of energy transfer is determined by the energy leakage into air, we next investigate the influence of size and shape of ENZ while keeping the resonance of the R-rod fixed. Equation (2) shows that $P_{\text{loss}}$ has no resonance behavior. Thus, near-unity energy transfer cannot be destroyed by varying the size of the ENZ region. In addition, the value of $P_{\text{loss}}$ decreases with the increase of $R_{\text{enz}}$, leading to transmission even closer to unity for a larger ENZ region. Importantly, this high efficiency is robust against arbitrary shapes of ENZ materials. Due to the nature of outgoing waves in air, $\psi_{\text{air}}$ does not exhibit any resonance to generate high $P_{\text{loss}}$, the resonance behavior of R-rod ensures the nearly complete energy transmission independent of the shape of the ENZ. To verify this, we intentionally deform the shape of the ENZ to contain sharp features as shown in Figure 1b. By numerical simulation we show that the transfer efficiency remains high, which is consistent with the above discussion (Figure 1c, e). Complete energy transfer is observed in the resonance region at $\epsilon_2$=9.843+0.0016i, which is the same as the undeformed case in Figure 1a. As shown by Equations (1) and (2), the efficiency is determined by $\eta$ regardless of $H_z$, indicating that the efficiency is independent of S-rod parameters. This feature differs critically from conventional systems that require the source and the receiver to resonate at the working frequency to achieve high efficiency of wireless power transfer. We further implement the analysis on the stability against the variation of the shape of the receiver. Without matching the resonance of the source to the receivers, the energy transfer efficiency remains high in an ENZ medium, which dramatically enhances the stability of the WPT. We further implement the analysis on the stability against the variation of the shape of the receiver (as shown in Section S2, Supporting Information). A source with defects or deformation can also efficiently transfer power to the receiver at any distance within the ENZ region. The influence of deviation from the ENZ environment is also investigated and the results are summarized in Section S2 (Supporting Information). It is shown that a slight deviation would lead to non-uniform distribution of the magnetic field inside the ENZ and a significant drop in the efficiency of power transfer. This indicates that the uniformity of magnetic field in the ENZ materials plays a central role for achieving efficient energy transfer. Meanwhile, we also prove that a small loss of ENZ environment does not have a prominent influence, only slightly reducing the efficiency of power transfer when the receiver is on resonance. To quantify the stability against background fluctuations, we introduce a characteristic permittivity for the ENZ environment, denoted as $\epsilon_{\text{c}}$. As the $\epsilon$ of the environment varies from 0 to $\epsilon_c$, there is a certain level of degradation in the maximum efficiency. For example, to keep 85% of the maximum transmission (or 15% degradation), $\epsilon_{\text{c}}$ is determined to be 0.003.

## 3. Results and Discussion

To better visualize the power transfer inside ENZ materials, we study the power flow between the S-rod and R-rod inside the ENZ region. Previous studies show that power flow inside ENZ is analogous to ideal fluid, meaning that power flow is robust against the defects by smoothly bending around defects of arbitrary geometries.[39] However, in our case, the receiver (R-rod) is not lossless and therefore it serves as the sink of power inside. Under the ideal energy transmission condition as shown in **Figure 2**a, the power flux lines converge into the R-rod and there is negligible fringe of power flux lines into the free space. We also simulate another configuration with randomly positioned R-rod and S-rod, which exhibits similar behavior, as shown in Figure 2b. Although close to the boundary of ENZ region, there is still little energy loss in the air, which indicates the full energy transfer from S-rod to R-rod. The uniform magnetic field distribution is observed in the ENZ region, which plays an important role in realizing the full transmission. While the magnetic field in free space may be larger than the field in the ENZ region, it is significantly smaller than the field within the receivers. This marked difference is a result of the resonance behavior, which enhances the field within the receivers and ensures efficient energy transmission. As comparison, we break the ENZ condition (increasing $\epsilon_{enz}$ to 0.01) and show the power flow in Figure 2c. A part of energy is coupled outside and the uniformity of the magnetic field in ENZ disappears. When the receiver approaches the boundary, more energy escape to the free space (as shown in in Figure 2d, leading

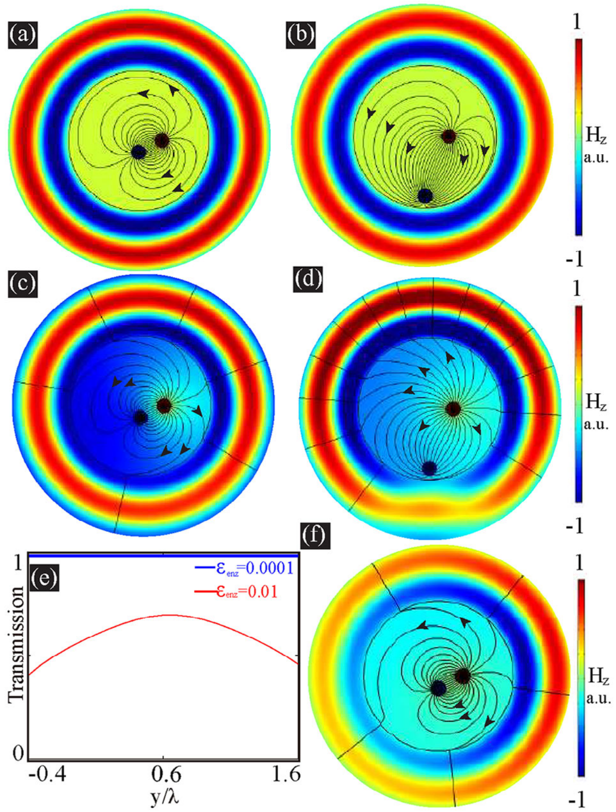


**Figure 2.** Investigation of the power transfer on dependence of ENZ condition. a,b) Normalized magnetic field and streamlines of the power in ENZ condition ($\epsilon_{enz} = 0.0001$) for two configurations of randomly positioned S-rod and R-rod. c,d) Normalized magnetic field and streamlines of the power in ENZ-broken condition for two randomly distributed configuration of S-rod and R-rod at $\epsilon_{enz} = 0.01$. e) The transmission with varying position of R-rod under ENZ and ENZ-broken condition, respectively. f) Normalized magnetic field and streamlines of the power in lossy-ENZ condition.

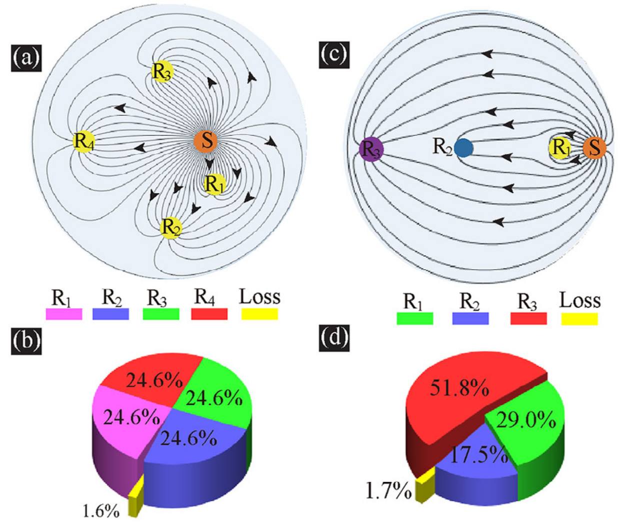


**Figure 3.** Energy Distribution with multiple receivers inside ENZ. a) Four identical receivers are placed at different distance from the source. The parameters are the same as Figure 1a. b) The percentage of energy acquired by each receiver from the source for (a). c) Three different receivers are placed inline. The $\epsilon$ of each receiver is 9.84-0.01i, 19.69-0.002i, 9.845-0.002i with radius 0.122$\lambda$, 0.086$\lambda$, 0.122$\lambda$, respectively. d) The percentage of energy received at each receiver from the source for (c).

to the efficiency degradation. The transfer efficiency in different positions is shown in Figure 2e. The x-axis is the position of R-rod along the y-direction. The corresponding transmission have verified the high efficiency for arbitrary position in ENZ region when ENZ condition preserves well. However, when the ENZ condition is broken, both advantages of position-independence and high efficiency are lost. Similarly, the loss of ENZ also breaks the uniform magnetic field, which is shown in Figure 2f.

With an increasing number of devices working simultaneously in a wireless network, it is important to be able to charge the local devices at equal proportion or at any desired proportions by WPT. Here, we show that ENZ provides a solution to distribute the energy at will, regardless of locations of the devices. Again, this salient feature can be attributed to the uniform magnetic field inside the ENZ region, which decouples the receivers from each other. To demonstrate equal energy distribution into multiple receivers, we place four identical receivers at arbitrary positions in the ENZ region, as shown in **Figure 3**a. The proportion of the energy each receiver acquires is plotted in Figure 3b. The uniform power distribution is manifested as the equal number of flux lines flowing into each receiver. The energy leakage into air is only 1.6%. This passive method for wireless power distribution would be much more energy-saving than the active methods. For distributing different powers to different receivers, one can simply manipulate the resonance frequencies of the receivers such that the receivers on resonance would acquire more energy. Because under the circumstance that ENZ region decouples the receivers from each other, from Equation (1) we calculate the energy different receivers get. The energy is dependent on the permittivity and radius of the receivers instead of the source and the position. By careful design of the relative size of each receiver, we can get the target energy distribution which is also position independent. The detailed steps is in Section S3 (Supporting Information). In the presence of the ENZ region that effectively decouples the receivers from each other, as demonstrated in Equation (1), we can calculate the energy distribution acquired by each receiver. Notably, this distribution is dependent on the permittivity and radius of the receivers rather than the source or their positions. Detailed steps for this process are provided in Section S3 (Supporting Information). To illustrate this, we design a system with three receivers and the targeted power proportions are 50:30:20. The locations of the three different receivers, are shown in Figure 3c and the corresponding realized energy distribution is in Figure 3d. Interestingly, although $R_3$ is the furthest, it acquires about half of the energy. $R_1$ acquires 29% of energy due to the slight deviation from the resonance condition, despite its proximity to the source.

Here, a simple structure consisting of two paralleled metallic circular plates is employed as the ENZ system, as shown in **Figure 4**a. It has been well established that the propagation of a TE mode at its cutoff frequency in this structure is equivalent to wave propagation inside a material with effective zero permittivity.[28–30] The separation of the two metallic plates in the z-axis is $H = \lambda_0/2$ corresponding to the cutoff frequency of $TE_1$

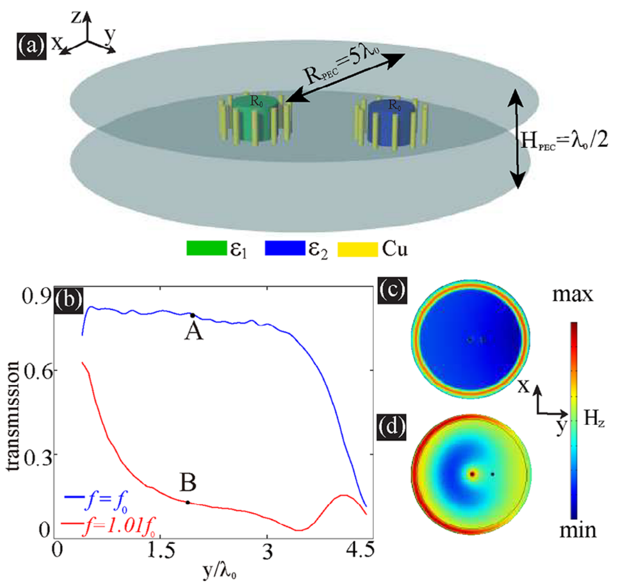


**Figure 4.** Proposed Experimental demonstration of high transmission inside ENZ system. a) Sketch of the proposed experiential setup. The structure consists of two metallic circular parallel plate whose separation is $\lambda_0/2$. Both receiver and source with a height equal to $\lambda_0/2$ are inserted inside the plates which are surrounded by ten metallic wires with a radius of 3.3 mm. The permittivity of the rod is $\epsilon_1$=10.84 and $\epsilon_2$=10.84-0.01i. The distance between them along the y-axis is y. b) The transmission with varying y at two working frequencies. c,d) The corresponding magnetic field in the ENZ region (except the rods) at A and B, respectively.

mode, where the operating wavelength $\lambda_0$ is 0.5m. The plates have a circular shape with $R_{ENZ} = 5\lambda_0$. Two dielectric rods with a height of $\lambda_0/2$ are used as the S-rod and R-rod, and placed at the center and on the y-axis, respectively. The permittivities of the S-rod and R-rod are $\epsilon_1$=10.84 and $\epsilon_2$=10.84-0.01i, respectively. This kind of materials is usually made by FR-4 glass epoxy. Both rods are surrounded by ten metallic wires, each with a radius of 3.3 mm. These metallic wires are used to suppress additional modes during the process of power transfer.[38] The radius of cross-section of the dielectric rods is $0.122\lambda_0$. To excite only the $TE_1$ mode, we place a magnetic line source along the z-axis at the center of S-rod that could be realized by small loop antenna. This forbids the excitation of TM modes that have a different symmetry. The efficiency of power transfer with varying distance between the two rods is shown in Figure 4b. We find that the efficiency is high over a broad range of distance. The decrease of efficiency for $y/\lambda_0 > 3$ is caused by the fringe effect of the plates where the system cannot be viewed as an ENZ material anymore. If the radius of parallel plate is increased, the high-efficiency would be preserved over an even longer distance. Due to the nonuniform magnetic field between the plates, the efficiency of energy transfer is not close to 100% as in the ideal 2D ENZ configuration, but reasonably high efficiency can still be achieved (> 76%). We further clarify that ENZ is the dominant factor in high energy efficiency, instead of the confinement between two metallic plates that limits upward and downward radiation channels. To demonstrate that ENZ is indeed the dominant factor, we slightly increase the working frequency away from the ENZ condition (f=1.01$f_0$) and study the impact on energy transfer. The corresponding effective epsilon is 0.02. To ensure the R-rod is still on resonance at this frequency, we slightly modify its permittivity to $\epsilon_2$=10.55-0.01i, while leaving the geometry structure unchanged. The dependence of the efficiency of energy transfer over the distance is shown in Figure 4b. It is shown that, in contrast to the ENZ condition, the efficiency drops rapidly with the increase of distance. Figure 4c,d illustrates the distribution of the magnetic field in the center plane (z = H/2) for the configurations corresponding to points A and B in Figure 4b, respectively. In Figure 4c, the key signature of wave propagation inside ENZ is preserved, i.e., the magnetic field is uniform in phase and amplitude across the structure. In contrast, in Figure 4d, the nonuniform magnetic field confirms the breakdown of ENZ condition despite the very small deviation of the operating frequency. The efficiency of power transfer can be further enhanced by enclosing the ENZ environment with a PEC (perfect electric conductor) shell, thus eliminating leakage power into the air. However, this approach may not only increase costs but also block external signals. In practical applications, particularly for long-range, or far-field wireless power transfer (WPT), the open environment proposed here may be preferable.

## 4. Conclusion

In conclusion, we have proposed to use ENZ media for achieving efficient wireless power transfer, offering a flexible, robust, and distance-independent energy distribution. We demonstrate a nearly perfect power transmission when the receiver resonates at the operating frequency inside the ENZ region. The power distribution can be fully controlled by the shape and optical property of receivers, independent of the parameters of the emitter. Furthermore, the power transfer is ENZ protected, regardless of specific geometric and optical parameters, and immune to perturbations. This stands in sharp contrast to other methods reported previously.[8–19] However, these advantages are conferred by the unique properties of the ENZ region, which add additional complexity to the environment.

## Supporting Information

Supporting Information is available from the Wiley Online Library or from the author.

## Acknowledgements

Q.Y. and S.Z. acknowledged support from the Research Grants Council of Hong Kong (AoE/P-701/20, 17315522) and The New Cornerstone Science Foundation. J.S. acknowledged support from the National Natural Science Foundation of China (62275061) and the Natural Science Foundation of Heilongjiang Province (ZD2020F002).

## Conflict of Interest

The authors declare no conflict of interest.

## Author Contributions

S.Z. and C.L. designed research; Q.Y. and S.Z. performed research; Q.Y., Y.W, J.S., C.L., and S.Z. analyzed data; Q.Y., C.L., and S.Z. wrote the paper. All authors discussed the results.

## Data Availability Statement

The data that support the findings of this study are available from the corresponding author upon reasonable request.

## Keywords

epsilon near zero, metamaterials, wireless power transfer

Received: July 11, 2023
Revised: October 6, 2023
Published online:

[1] N. Tesla, *Electr.World Eng.* **1904**, *43*, 23760.
[2] J. S. Ho, S. Kim, A. S. Y. Poon, *Proc. IEEE* **2013**, *101*, 1369.
[3] J. Huang, Y. D. Zhou, Z. L. Ning, H. Gharavi, *IEEE Wireless Commun.* **2019**, *26*, 163.
[4] S. Y. R. Hui, W. X. Zhong, C. K. Lee, *IEEE Trans. Power Electron.* **2014**, *29*, 4500.
[5] C. T. Rim, C. Mi, *Dynamic Charging for Road-Powered Electric Vehicles (RPEVs)*, Wiley-IEEE Press, Hoboken **2017**, pp. 153–153.
[6] M. Z. Song, P. Belov, P. Kapitanova, *Appl. Phys. Rev.* **2017**, *4*, 2.
[7] M. Z. Song, P. Jayathurathnage, E. Zanganeh, M. Krasikova, P. Smirnov, P. Belov, P. Kapitanova, C. Simovski, S. Tretyakov, A. Krasnok, *Nat. Electron.* **2021**, *4*, 707.
[8] A. Kurs, A. Karalis, R. Moffatt, J. D. Joannopoulos, P. Fisher, M. Soljacic, *Science* **2007**, *317*, 83.
[9] S. Assawaworrarit, X. F. Yu, S. H. Fan, *Nature* **2017**, *546*, 387.
[10] H. Cui, Z. Dong, H.-J. Kim, C. Li, W. Chen, G. Xu, C.-W. Qiu, J. S. Ho, *Phys. Rev. Appl.* **2022**, *18*, 044076.
[11] J. Schindler, A. Li, M. C. Zheng, F. M. Ellis, T. Kottos, *Phys. Rev. A* **2011**, *84*, 4.
[12] Y. Wu, L. Kang, D. H. Werner, *Phys. Rev. Lett.* **2022**, *129*, 200201.
[13] F. Liu, B. Chowkwale, P. Jayathurathnage, S. Tretyakov, *Phys. Rev. Appl.* **2019**, *12*, 5.
[14] Y. Ra'di, B. Chowkwale, C. Valagiannopoulos, F. Liu, A. Alu, C. R. Simovski, S. A. Tretyakov, *IEEE Trans. Antennas Propag.* **2018**, *66*, 4260.
[15] S. C. Li, F. Sun, D. An, S. L. He, *IEEE Trans. Power Electron.* **2018**, *33*, 3325.
[16] J. Prat-Camps, C. Navau, A. Sanchez, *Appl. Phys. Lett.* **2014**, *105*, 23.
[17] J. Prat-Camps, C. Navau, A. Sanchez, *Adv. Mater.* **2016**, *28*, 4898.
[18] A. K. Baghel, S. S. Kulkarni, S. K. Nayak, *IEEE Microw. Wirel. Compon. Lett.* **2019**, *29*, 424.
[19] A. Hajimiri, B. Abiri, F. Bohn, M. Gal-Katziri, M. H. Manohara, *IEEE J. Solid-State Circuits* **2021**, *56*, 2077.
[20] M. Dubois, C. Z. Shi, X. F. Zhu, Y. Wang, X. Zhang, *Nat. Commun.* **2017**, *8*, 14871.
[21] X. Q. Huang, Y. Lai, Z. H. Hang, H. H. Zheng, C. T. Chan, *Nat. Mater.* **2011**, *10*, 582.
[22] I. Liberal, N. Engheta, *Nat. Photonics* **2017**, *11*, 149.
[23] P. Moitra, Y. M. Yang, Z. Anderson, I. I. Kravchenko, D. P. Briggs, J. Valentine, *Nat. Photonics* **2013**, *7*, 791.
[24] J. C. Soric, N. Engheta, S. Maci, A. Alu, *IEEE Trans. Antennas Propag.* **2013**, *61*, 33.
[25] Z. Y. Wang, F. Yang, L. B. Liu, M. Kang, F. M. Liu, *J. Appl. Phys.* **2013**, *114*, 19.
[26] C. Q. Xu, G. C. Ma, G. Chen, J. Luo, J. J. Shi, Y. Lai, Y. Wu, *Phys. Rev. Lett.* **2020**, *124*, 7.
[27] Z. H. Zhou, Y. Li, H. Li, W. Y. Sun, I. Liberal, N. Engheta, *Nat. Commun.* **2019**, *10*, 4132.
[28] B. Edwards, A. Alu, M. E. Young, M. Silveirinha, N. Engheta, *Phys. Rev. Lett.* **2008**, *100*, 3.
[29] R. Fleury, A. Alu, *Phys. Rev. Lett.* **2013**, *111*, 5.
[30] M. Silveirinha, N. Engheta, *Phys. Rev. Lett.* **2006**, *97*, 15.
[31] O. Reshef, P. Camayd-Munoz, D. I. Vulis, Y. Li, M. Loncar, E. Mazur, *Acs Photonics* **2017**, *4*, 2385.
[32] J. M. Hao, W. Yan, M. Qiu, *Appl. Phys. Lett.* **2010**, *96*, 10.
[33] C. Argyropoulos, P. Y. Chen, G. D'Aguanno, N. Engheta, A. Alu, *Phys. Rev. B* **2012**, *85*, 4.
[34] I. Liberal, N. Engheta, *Proc. Natl. Acad. Sci. USA* **2017**, *114*, 822.
[35] Y. Z. Cheng, J. Jin, W. L. Li, J. F. Chen, B. Wang, R. Z. Gong, *Aeu-Inter. J. Electron. Commun.* **2016**, *70*, 1282.
[36] G. Lipworth, J. Ensworth, K. Seetharam, D. Huang, J. S. Lee, P. Schmalenberg, T. Nomura, M. S. Reynolds, D. R. Smith, Y. Urzhumov, *Sci. Rep.* **2014**, *4*, 3642.
[37] J. Prat-Camps, C. Navau, A. Sanchez, *Appl. Phys. Lett.* **2014**, *105*, 23.
[38] I. Liberal, A. M. Mahmoud, Y. Li, B. Edwards, N. Engheta, *Science* **2017**, *355*, 6329.
[39] I. Liberal, M. Lobet, Y. Li, N. Engheta, *Proc. Natl. Acad. Sci. USA* **2020**, *117*, 24050.